INSTITUT FÜR PLASMAPHYSIK

GARCHING BEI MÜNCHEN

On Diffusion in the Garching Octopole Device

H. Grawe

IPP 6/61 October 1967

Die nachstehende Arbeit wurde im Rahmen des Vertrages zwischen dem Institut für Plasmaphysik GmbH und der Europäischen Atomgemeinschaft über die Zusammenarbeit auf dem Gebiete der Plasmaphysik durchgeführt.

IPP 6/61 H. Grawe On Diffusion in the Garching Octopole Device.

October, 1967 (in English)

ABSTRACT:

Previous papers [1), 2)] on the octopole experiments treated the various loss mechanisms in the octopole device as independent of each other. In addition to diffusion across the magnetic field the loss flux along $\underline{B}$ to the supports of the ring conductors generating the field is important. In this paper these two loss mechanisms are taken into account simultaneously. Smearing out the loss flux along $\underline{B}$ around the machine we get a simple differential equation for this loss, which is solved numerically together with a diffusion equation. Postulating FICK's law describing the diffusion we approximate the measured density profile by varying the diffusion coefficient. The best approximating coefficient is between resistive and Bohm diffusion but tends more to Bohm diffusion. Owing to the large ion gyroradii in the inner part of the machine we consider ion-ion collisions, too. The diffusion equation obtained from this mechanism describes the measured profile very well, but does not lead to a unique relation between the adjusted flux from the particle source and the peak particle density for the operating regime.

In a paper presented at the Culham Conference, 1965, D. ECKHARTT et al.[1] reported on diffusion measurements obtained in the WENDELSTEIN stellarator and in a toroidal octopole device. In both devices the confinement of a low-β caesium plasma was investigated under conditions such that the plasma could be considered as quiescent and in thermal equilibrium. For the stellarator the measured density profile was compared with a theoretical profile calculated from FICK's law taking into account the losses due to recombination on the ceramic tube supporting the plasma source, whereas for the octopole device only rough estimates of the plasma losses were given. In this paper similar calculations to those for the stellarator are made for the octopole device in order to decide whether or not purely resistive diffusion can explain the measured density profile.

A schematic drawing of the field pattern in the octopole device is shown in Fig. 1, which is to be imagined as completed by rotational symmetry around the axis s = 0 and by mirror symmetry around the plane z = 0. Four ring-shaped conductors carrying currents in the same direction generate this purely meridional field B_M. Current and cooling water are fed to each ring conductor through one support; another two supporting rods keep the ring in position. In the experiment a small azimuthal magnetic field B_L is superimposed, but it is neglected in our calculations. The critical field line ψ_c encloses a flute-stable volume, where $\nabla p \cdot \nabla \oint \frac{dl}{B} > 0$ The caesium plasma is produced by contact ionization on a piece of tantalum metal (15 mm in diam.) located in the plane $z = 0$ on the separatrix ψ_0 (at radial distance $s = 41.2$ cm), where $B_M = 0$. There is another separatrix ψ_0' on both sides of the plane of symmetry. These separatrices divide half a meridional plane in four parts I, II, III, IV (see Fig. 1). The field lines in I encircle all four ring conductors, those in IV encircle the pair of ring conductors above the plane $z = 0$, whereas in II and III the field lines encircle only one ring conductor.

In a previous report [2] D. ECKHARTT et al. compared various loss mechanisms in the octopole device:

a.) Particle diffusion to the outer walls and to the surfaces of the inner ring conductors.

b.) Volume recombination

c.) Losses due to recombination on the hot Ta-plate and its supports

d.) Losses due to collisions with neutral atoms including charge transfer

e.) Losses due to recombination on the supports of the ring conductors.

Treating these particle losses as independent of each other they concluded that a) and e) are the main loss mechanisms, compared with which b), c), d) are negligible in the operating regime of the experiment. The purpose of this paper is to take into account a) and e) simultaneously.

In order to do this some more or less obvious simplifications are made. First we postulate that the temperature of the plasma be uniform and isotropic. We define a magnetic surface in this device by the rotation of a magnetic field line around the z-axis and we assume the magnetic surface generated by the separatrix ψ_o as a surface-source around the machine. This assumption is justified by the fact that the Ta-plate is located on ψ_o and the plasma spreads in the azimuthal and meridional directions with thermal velocity

v_{th} (5 x 10^4 cm/sec; also in the azimuthal direction because of the small azimuthal field B_ι) and with drift velocity v_D , which is not much smaller than v_{th} ; this is because in a large part of the device the curvature radii of the field lines are only a few times the gyroradii of the caesium ions. Later, in Chapter A, we shall smear out the recombination on the supports over the whole volume of the device. Together with the above assumption this leads to the conservation of rotational symmetry. If inertia terms are neglected, there can in equilibrium be no pressure gradient along the magnetic lines, and so the magnetic surfaces are surfaces of equal density.

A. Loss flux to the supports of the ring conductors.

As mentioned above, each ring conductor is supported by three rods. Thus each magnetic surface is intersected by several supports, the number depending on the field zone (I, II, III, IV) to which the considered surface belongs. Let us enumerate the supports by the index μ. We calculate the particle loss flux to these supports in the same way as done in [2] and [3] by using a simplified single particle picture instead of solving the diffusion problem near the supports. The mean free path for ion-electron collisions

$$\lambda_{ie} = \tau_{ie} \cdot v_{th} = \frac{3.1 \times 10^{13}}{n} \quad cm$$

(for Cs with $E_{th} = 0{,}2$ eV) is large compared with all linear dimensions of the machine in the density range of interest ($n \approx 10^9$ cm^{-3}). Thus with a recombination probability 1 the particle loss on the supports is simply the thermal ion flux to them. This flux in a shell between the magnetic surface ψ_1 and ψ_2 is

(1)
$$\Delta\Phi = -\frac{1}{4} v_{th}\, n\, 2 \sum_{\mu} b_{\mu} \Delta\xi_{\mu}$$

n is the particle density on ψ_1, $\Delta\xi_\mu$ is the infinitesimal distance of ψ_2 from ψ_1 at the spot of the support number μ, b_μ is the effective width of this support in the azimuthal direction. The supporting tubes are of rectangular cross section with the linear dimension d_μ in the azimuthal direction and a_μ parallel to the magnetic field. If the gyroradius of the ions $r_{g\mu}$ at the support under consideration is smaller than a_μ, we assume that the surface of the support is reached by all particles, whose guiding centres lie inside a magnetic flux tube of width equal to the breadth d_μ of the support plus one radius of gyration on either side. If the gyroradius is larger than a_μ we take for the effective width b_μ half the circumference of the support

(2) $$b_\mu = \min \left\{ \begin{matrix} d_\mu + a_\mu \\ d_\mu + 2 r_{g\mu} \end{matrix} \right\}$$

In order to get from (1) a differential equation for the particle flux ϕ we have to replace $\Delta \xi_\mu$ by Δx, where x is the coordinate along an arbitrary but fixed line normal to the ψ -surfaces. We denote the radial distance from the axis of the machine by s and all quantities along the special coordinate x by a lower index 0. Then from $\nabla \underline{B} = 0$ it follows that

(3) $$B_0 s_0 dx = B s d\xi$$

B , s , $d\xi$ are the quantities as defined above at an arbitrary point on the same magnetic surface where B_0, s_0 , dx are taken. From (1) and (3) we get the differential equation (replacing ϕ_0 , n_0 by ϕ and n)

(4) $$\frac{d\phi}{dx} = - P(x)\, n$$

(5) $$P(x) = \frac{1}{2} B_0(x)\, s_0(x)\, v_{th} \sum_\mu \frac{b_\mu}{B_\mu s_\mu}$$

For the zone I x is chosen in the plane z = 0 from the separatrix ψ_0 to the axis s = 0, i.e. x = -s. The dependence of P on s is shown in Fig. 2, the measured density profile is given, too. The experiments were made for three different field strengths, but the density profile was given in [1)] only for the lowest field, our results for which are reported in this paper. In these three cases the geometric pattern of the field lines is the same, but the field strength B_{max} at a fixed point near the inner ring conductor is in the different cases (which we characterize by the factor α):

$$B_{max} = 1.3 \ k\Gamma \quad \hat{=} \quad \alpha = 0.1$$
$$= 2.6 \ k\Gamma \quad \hat{=} \quad \alpha = 0.2$$
$$= 3.9 \ k\Gamma \quad \hat{=} \quad \alpha = 0.3$$

P is different for these three cases only because of the appearance of the gyroradii in (2). P grows very strongly as s decreases, because the ratio B_o/B_p grows by a factor of ten from s = 40 cm to s = 26.5 cm. This is the reason why for the measured density profile the loss flux to the supports is only half the loss flux resulting when taking n = const = 7×10^8 cm^{-3} from s = 40 to s = 31, as shown in Fig. 3. The s-dependence of Φ in Fig. 3 is obtained by integrating eq. (4) assuming n = const for the lower curve in Fig. 3 and the measured density profile for the upper curve. In both cases the boundary value on the separatrix ψ_o for the flux to the walls is taken as $\Phi_{wo} = 2 \times 10^{15}$ sec^{-1} for α = 0.1.

Choosing this boundary value is a major difficulty in calculating the density profile. This is because, although the complete flux Φ_{co} from the plasma source was measured, no information exists on what portion Φ_{wo} of this flux diffused to the wall and what portion Φ_{ro} diffused to the ring conductors. Moreover, the density profile for the inner zones II, III, IV was not measured. Therefore, in principle, two methods of approximating the measured density profile in I exist . Firstly, we postulate a fixed diffusion coefficient (e.g. D_{rc}) and try to find the flux Φ_{wo} , which can be driven from ψ_o to the wall by the assumed diffusion mechanism (taking into account the loss flux to the supports). For resistive diffusion this is done in section B1. Secondly, we estimate the loss flux in the innner zones Φ_{ro} and ask what diffusion mechanism leads to the best approximation of the measured density profile if we take the flux to the wall fixed as $\Phi_{wo} = \Phi_{oo} - \Phi_{ro}$.

In order to get an estimate for Φ_{ro} we have to consider the gyroradii in the inner zones of the separatrix ψ_0 . For a mean point in zone III (z = 15.5; s = 58.0) the gyroradius is

$$r_g = \frac{0.17}{\alpha} \text{ cm}$$

wheras the breadth δ of the zone (see Fig. 1) is 1 cm. Therefore, if there had not been an electrostatic sheath on the ring conductors the confinement time would have been of the order of the period of gyration

$$\omega_g^{-1} = \frac{1}{\alpha} \times 3 \times 10^{-6} \text{ sec} \quad (\text{for } z = 15.5; \; s = 58.0)$$

In [2] the experimentally considered confinement time was estimated by $\tau = n_o V / \Phi_{oo}$ with n_o being the peak value of the measured density and V the plasma volume given as

$$V \approx 1.25 \times 10^5 \text{ cm}^3$$

With $n_o = 7 \times 10^8 \text{ cm}^{-3}$, $\Phi_{oo} = 2.6 \times 10^{15} \text{sec}^{-1}$

it follows that

$$\tau_{exp} = 3.4 \times 10^{-2} \text{sec}$$

This leads to the assumption that an electric sheath exists on the ring conductors and the electrons govern the diffusion across the magnetic field lines. Assuming a constant particle flux perpendicular to the magnetic field in the zone III and a decrease of the particle density from its peak value n_o on the separatrix to $n = 0$ on the ring conductors, we get from the diffusion equation (10) an estimate for the particle flux driven by resistive diffusion from the surface source to the ring conductor 2 :

$$\phi_{r2} = \frac{n_o^2}{\delta \alpha^2 \overline{Q}} = 2 \times 10^{-7} \times \frac{n_o^2}{\alpha^2}$$

(For the definition of Q see section B) A mean value $\overline{Q}$ of Q for the zone II as well as for zone III is

$$\overline{Q} = 5 \times 10^{6} \text{ cm}^{-7} \text{ sec}$$

Thus the particle flux across the magnetic field to all four ring conductors is less than

$$\phi_r = 4 \times 10^{13} \text{ sec}^{-1}$$

and ϕ_r is negligible relative to ϕ_∞ . Choosing $n = \text{const} = n_o$ in the whole inner region of ψ_o , we get a maximum flux $\phi_{i,\,max}$ to the supports in this region by integrating (4) along a straight line z = 15.5 with $\overline{P}$ a mean value of P in II, III, and IV.

$$\phi_{II\,max} = \overline{P}_{II}\, n_o\, (26.7 - 26.3) = 5.3 \times 10^{13} \text{ sec}^{-1}$$

$$\phi_{III\,max} = \overline{P}_{III}\, n_o\, (58.0 - 57.3) = 8.4 \times 10^{13} \text{ sec}^{-1}$$

$$\phi_{IV\,max} = \overline{P}_{IV}\, n_o\, (58.2 - 58.0) = 4.5 \times 10^{13} \text{ sec}^{-1}$$

(6) $$\phi_{i,max} = 2\,(\phi_{II\,max} + \phi_{III\,max} + \phi_{IV\,max}) = 3.6 \times 10^{14} \text{ sec}^{-1}$$

B.1. Resistive diffusion

If we denote the diffusion coefficient by D_{κ} , the particle flux ϕ through a magnetic surface is given by

(7) $$\phi = - 2\pi \oint D_{\kappa} \, |\nabla_{\perp} n| \, s \, dl$$

Using Gaussian units and expressing E_{th} in eV we can write the diffusion coefficient

(8) $$D_{\kappa} = A_{\kappa} \frac{n}{B^2} C_{\kappa}$$

with

$$A_{\kappa} = 1.65 \times 10^{-5} \times \frac{\ln \Lambda}{\sqrt{E_{th}}} \approx 1.7 \times 10^{-4} \times \frac{1}{\sqrt{E_{th}}}$$

for $\ln\Lambda \approx 10$. C_{κ} is a dimensionless factor introduced for approximating the diffusion coefficient best. For $C_{\kappa} = 1$ the coefficient for classical diffusion follows. The integral in (7) has to be taken along the closed line of force by which the considered magnetic surface is generated, and $\nabla_{\perp} n$ is the component of ∇n perpendicular to this surface. We introduce ξ as a coordinate in this direction at an arbitrary point on the considered field line and x as the same coordinate at a fixed point characterized by the index 0 and given by the intersection of the field line with the integration path for our differential equations (For part I the straight line $z = 0$). The magnetic surfaces are surfaces of constant density. This means that

(9) $$\nabla_{\perp} n_0 \, dx = \nabla_{\perp} n \, d\xi$$

And because of (3) it follows that

$$\Phi = -2\pi \cdot A_{rc}\, n_c \, (\nabla_\perp n)_o \, \frac{1}{B_c S_o} \oint \frac{s^2}{B} \, dl$$

From these equations together with

$$n_o (\nabla_\perp n)_o = \frac{1}{2} \; \frac{d}{dx} n^2$$

we obtain the differential equation (rewriting n instead of n_o)

(10) $$\frac{d}{dx} n^2 = -\alpha^2 \; Q(x) \; \Phi$$

(11) $$Q(x) = \frac{\bar{B}(x) \; x}{\pi \, C_{rc} \, A_{rc}} \left[\oint \frac{s^2}{\bar{B}} \, dl \right]^{-1}$$

where $\bar{B}$ is the reference field for α = 1. A drawing of Q(x) for zone I (along z = 0) with C_{rc} = 1 is given in Fig. 4. Q decreases very strongly from s = 26.5 to 40.0, because $\bar{B} \approx 3.3\ k\Gamma$ for s = 26.5 and $\bar{B} \approx 0.12\ k\Gamma$ for s = 40.0, whereas $\oint s^2/\bar{B}\ dl$ only grows by a factor 2 from 26.5 to 40.0. At first we assume C_{rc} = 1, i.e. purely classical diffusion and vary the boundary value Φ_{wo} for Φ at s = 40.0 integrating the equations (4) and (10) for α = 0.1 and choosing the boundary value for n as the measured value n_o = 7 x 10^8 cm^{-3}. The result is shown in Fig. 5. For Φ_{wo} = 1.5 x 10^{15} sec^{-1} (the measured total flux from the source was Φ_{ou} = 2.6 x 10^{15}) the density gradient ought to be much greater than that measured in order to drive the flux by resistive diffusion to the walls. Even for $\phi_{wo} = 2 \times 10^{14}$ the calculated profile is much narrower than the measured one. Therefore purely resistive diffusion could explain the measured density profile only if there were a good reason for assuming a loss flux of more than 90 percent of ϕ_{oo} inside the separatrix ψ_o .

Thus we now calculate the factor C_{re} by which $\mathcal{D}_{re}$ must be multiplied to approximate the measured density profile, ϕ_{wo} being taken as fixed. According to the estimates given in section A we choose

$$\phi_{wo} = 2 \times 10^{15} \text{ sec}^{-1} \quad \text{for } \alpha = 0.1$$

For $n_o = 7 \times 10^{8}$ cm^{-3} the results are given in Fig. 6a. The breadth of the profile is approximately that measured for $C_{re} = 28$. For this profile the flux ϕ_w to the wall is given, too. It is 80 - 90 percent of ϕ_{wo} . In order to investigate the influence of a variation of n_o on the factor C_{re} we need, we made the same calculations for lower values of n_o . For $\alpha = 0.1$ such values of n_o were not really measured, but let us make the hypothesis that the probes would have detected a density too high by, say, a factor 2. As may be seen from Figs. 6b and 6c the breadth of the density profile depends strongly on the choice of n_o . For $n_o = 3.5 \times 10^{7}$ cm^{-3} we need $C_{re} \gtrsim 100$ and for $n_o = 1 \times 10^{7}$ cm^{-3} the profile is much too narrow even for $C_{re} = 100$. This dependence is obvious because eq. (10) is quadratic in n . The results are compiled together with those for Bohm diffusion in Table 1.

n_0 [cm^{-3}]	Φ_{w0} [sec^{-1}]	$D_\perp$	Φ_w [sec^{-1}]
7×10^8	2×10^{15}	$28 \times D_{rc}$	1.78×10^{15}
		$\frac{1}{30} \times D_B$	1.70×10^{15}
3.5×10^8	2×10^{15}	$\gtrsim 100 \times D_{rc}$	1.9×10^{15}
		$\frac{1}{15} \times D_B$	1.85×10^{15}
1×10^8	2×10^{15}	$\gg 100 \times D_{rc}$	?
		$\frac{1}{4} \times D_B$	1.96×10^{15}

T a b l e 1

B.2. Bohm diffusion

As for resistive diffusion we start with eq. (7). But now the diffusion coefficient is given by

(12) $$D_B = \frac{A_B}{B} C_B$$

with

$$A_B = 6.25 \times 10^6 \times E_{th} \quad (E_{th} \text{ in eV})$$

Again C_B is a dimensionless factor for varying the diffusion coefficient. Going on in the same way as for resistive diffusion we get for Bohm diffusion the differential equation

(13) $$\frac{dn}{dx} = -\alpha \cdot R(x)\,\Phi$$

(14) $$R(x) = \frac{\overline{B}(x)\, X}{2\pi A_B C_B}\left[\oint s^2\, dl\right]^{-1}$$

For zone I a drawing of R(x) with $C_B = 1$ is given in Fig. 7. Again the strong dependence on s is caused by that of $\overline{B}$. For the integration of eqs. (13) and (4) we take the boundary value for Φ as fixed:

$$\Phi_{wo} = 2 \times 10^{15}\ \text{sec}^{-1} \quad \text{for} \quad \alpha = 0.1$$

For $n_o = 7 \times 10^8\ \text{cm}^{-3}$ the results are given in Fig. 9a. Pure Bohm diffusion ($C_B = 1$) is much too fast and leads to a density profile of almost constant density from s = 40 to s = 31. The measured diffusion is about a factor of 30 slower than Bohm diffusion. But for the hypothetical peak density $n_o = 3.5 \times 10^7\ \text{cm}^{-3}$ we need only $C_B = \frac{1}{15}$ for approximating the experimentally detected profile and for $n_o = 1 \times 10^7\ \text{cm}^{-3}$ only $C_B = \frac{1}{4}$ is necessary. Therefore if the measured density happens to be a factor of only 2 higher than it really is, the diffusion is much nearer to Bohm diffusion than to resistive diffusion, as may be seen from Table 1.

C. Diffusion due to Like Particle Collisions

Considering the density profiles calculated above one sees that FICK's law does not lead to a density plateau as detected by the measurements. Therefore one supposes a higher order differential equation describing the diffusion mechanism. Moreover, in the region of this plateau the gyroradii are large compared with the scale length of the density gradient. About ten years ago SIMON[4] as well as ROSENBLUTH and LONGMIRE[5] stated that diffusion due to ion-ion collisions is no longer negligible compared with diffusion due to electron-ion collisions, if the gyroradii are large. SIMON gave the particle flux due to ion-ion collisions as

$$\phi_{ii} = \frac{3}{8} \frac{r_{gi}^4}{\tau_{ii}} n \nabla_\perp \left(\frac{1}{n} \nabla_\perp^2 n \right)$$

r_{gi} is the gyroradius of the ions, τ_{ii} the ion-ion collision time. If we assume equal mean free paths for ion-ion and ion-electron collisions and if we introduce q as the characteristic length of the density gradient, the ratio of the particle flux across the magnetic field due to ion-ion collisions and the flux due to ion-electron collisions is given by

$$\left| \frac{\phi_{ii}}{\phi_{R}} \right| = \frac{3}{4} \left(\frac{m_i}{m_e} \right)^{\frac{1}{2}} \cdot \left(\frac{r_{gi}}{q} \right)^2$$

Thus ϕ_{ii} might be important particularly in the case of heavy ions like caesium.

Combining resistive diffusion and diffusion due to like particle collisions we obtain the flux perpendicular to the magnetic field

(15) $$\phi = -2\pi \oint D_{\kappa} (\nabla_{\perp} n)\, s\, dl + 2\pi \oint D_{ii} (\nabla_{\perp} \tfrac{1}{n} \nabla_{\perp}^{2} n)\, s\, dl$$

Again the integrals are to be taken along a closed magnetic field line, D_{κ} is given in (8), D_{ii} is defined by

(16) $$D_{ii} = A_{ii} \frac{n^{2}}{B^{4}}$$

(17) $$A_{ii} = \frac{3}{8} \frac{1}{\tau_{ii}\, n} \left(\frac{V_{th}\; m_i\; c}{e} \right)^{4} = A_{\kappa} \left(\frac{V_{th}\; m_i\; c}{e} \right)^{2} \frac{3}{4} \left(\frac{m_i}{m_e} \right)^{\frac{1}{2}}$$

In the second integral on the right-hand side of (15) we handle the differentiation in a similar manner to that above for the first integral. We recall that ξ was a coordinate perpendicular to the considered magnetic surface at an arbitrary point of the field line but that x was the same coordinate in the intersection point of the field line and the integration path for the differential equations. Then we have

$$\nabla_{\perp} n = \frac{dn}{dx} \frac{dx}{d\xi}$$

and from (3)

(18) $$\frac{dx}{d\xi} = \frac{B\, s}{B_0\, s_0}$$

(19a) $$\nabla_{\perp}^{2} n = \frac{d^{2} n}{d x^{2}} \left(\frac{dx}{d\xi} \right)^{2} + \frac{dn}{dx} \frac{d^{2} x}{d \xi^{2}}$$

(19b) $$\nabla_\perp^3 n = \frac{d^3 n}{dx^3}\left(\frac{dx}{d\xi}\right)^3 + 3\,\frac{d^2 n}{dx^2}\,\frac{dx}{d\xi}\,\frac{d^2 x}{d\xi^2} + \frac{dn}{dx}\,\frac{d^3 x}{d\xi^3}$$

We can easily transform the first term on the right-hand side of (19a) and (19b) using (18). The other terms we shall neglect. This is because $\frac{dx}{d\xi}$ describes the ratio of the distance of two infinitesimally neighbouring magnetic surfaces, if we measure this distance once along the coordinate x and once along ξ . Therefore $\frac{d^2x}{d\xi^2}$ represents the change of this ratio going along the coordinate ξ from one surface to a neighbouring one. From Fig. 1 it is obvious that this change is not important. Thus from (16), (18), (19) we get for the last term on the right-hand side of (15)

$$\oint D_{ii}\left(\nabla_\perp \frac{1}{n}\nabla_\perp^2 n\right) s\, dl \approx A_{ii}\, n^2 \frac{d}{dx}\left(\frac{1}{n}\frac{d^2}{dx^2}n\right)\oint \frac{1}{B^4}\left(\frac{dx}{d\xi}\right)^3 s\, dl$$

$$= n^2 \frac{d}{dx}\left(\frac{1}{n}\frac{d^2}{dx^2}n\right)\frac{A_{ii}}{B_0^3\, s_0^3}\oint \frac{s^4}{B}\, dl$$

For the flux ϕ it follows that

$$\phi = -\left(\frac{\pi A_{ie}}{B_0\, s_0}\right)\left\{\frac{dn^2}{dx}\oint\frac{s^2}{B}\,dl - \frac{2}{\alpha^2\, T\, s_0^2}\, n^2\frac{d}{dx}\left(\frac{1}{n}\frac{d^2}{dx^2}n\right)\oint\frac{s^4}{B}\,dl\right\}$$

T is defined by

$$T(x) = \frac{4}{3}\left(\frac{m_e}{m_i}\right)^{\frac{1}{2}}\,\bar{r}_{gi}^{\,-2}(x)$$

If we assume

$$\frac{1}{s_0^2}\oint\frac{s^4}{B}\,dl \approx \oint\frac{s^2}{B}\,dl$$

only the well known Q appears. Thus we get the differential equation

$$2 n^2 \left(\frac{d}{dx} \frac{1}{n} \frac{d^2}{dx^2} n \right) - \alpha^2 T(x) \frac{d}{dx} n^2 = \alpha^4 T(x)\, Q(x)\, \Phi \tag{20}$$

For section I T(x) is given in Fig. 8. Like Q(x) it grows strongly for diminishing s. Therefore for s near s = 40 cm the density profile is expected to be nearly exponential, because the first term on the right-hand side of (20) vanishes for an exponential density profile. Equation (20) was integrated along the straight line z = 0 together with eq. (4). But then we had a free choice of two more boundary values, namely n' and n''. According to the density measurements n' was postulated to be zero at s = 39.5 cm, whereas varying n'' we obtained a set of curves and chose that curve which best approximates the measured density profile. The results are shwon in Fig. 10. The most surprising result is less obvious from Fig. 10: If we calculate the best approximating profile for $\Phi_{wo} = 4 \times 10^{14}\ sec^{-1}$ instead of $\Phi_{wo} = 2 \times 10^{15}\ sec^{-1}$, the resulting curve is unchanged in terms of the calculating accuracy except for the density value for s = 31.0. This very insensitive dependence on Φ_{wo} is due to the very small factor $\alpha^4 T Q$ by which Φ is multiplied in (20). The behaviour of the calculated profile is governed by the homogeneous part of (20) in the operating regime of the experiment. Thus equation (20) does not lead to a unique relation between the peak particle density n_o and the particle flux from the source Φ_{wo}. Experimentally such a relation was found. For this reason we do not believe that the diffusion in the octopole device is governed by like particle collisions, although this diffusion mechanism best approximates the measured density profile.

D. Conclusions

Summarizing our results we must state that the measurements made hitherto do not provide a definite answer to the question of the diffusion mechanism.+) In particular, measurements relating to the inner part of the separatrix ψ_0 are missing. But if we assume, as was justified in section A, that the only loss flux inside ψ_0 is along the magnetic lines of force to the supports and the flux perpendicular to $\underline{B}$ to the ring conductors is negligible, the measured density profile allows two interpretations. Either FICK's law governs the diffusion and the diffusion coefficient is between pure resistive and pure Bohm Diffusion but tends more to Bohm diffusion, or diffusion due to ion-ion collisions is partly responsible for the particle flux perpendicular to $\underline{B}$ and the diffusion is purely classical. But the latter alternative does not lead to a unique relation between the peak particle density and the adjusted flux Φ_{oc} from the particle source. The loss flux along $\underline{B}$ to the supports of the ring conductors is not so important as estimated by ECKHARTT et al. . According to our calculations this flux outside ψ_0 is only about 10% of Φ_{cc} and for the whole machine less than 25% of Φ_{cc} . The rest flux is driven to the walls.

Acknowledgements

Previous calculations of the magnetic field lines and the various integrals along them performed by Dr. K.U. v. Hagenow have been used here. The author would like to thank Dr. D. Eckhartt, Dr. G. v. Gierke and Dr. G. Grieger for helpful discussions. He is most indebted to W. Stodiek for his clarifying remarks.

+) It is fairly certain, however that pump-out losses (i.e. C_B = 1) do not occur.

References

1) D. Eckhartt, G. v. Gierke, G. Grieger:
In Proceedings of a Conference on Plasma Physics and Controlled Nuclear Fusion Research, Culham, England, 1965; Vol. II p. 718

2) D. Eckhartt, G. v. Gierke, G. Grieger:
Report Max-Planck-Institut für Physik und Astrophysik, Munich, MPI-PAE/Pl. 6/65

3) R.A. Dory, D.W. Kerst, D.M. Meade, W.E. Wilson, C.W. Erickson:
Phys. Fluids 9, 997 (1966)

4) A. Simon:
Phys. Rev. 100, 1557 (1955)

5) M.N. Rosenbluth, C.L. Longmire:
Phys. Rev. 103, 507 (1956)

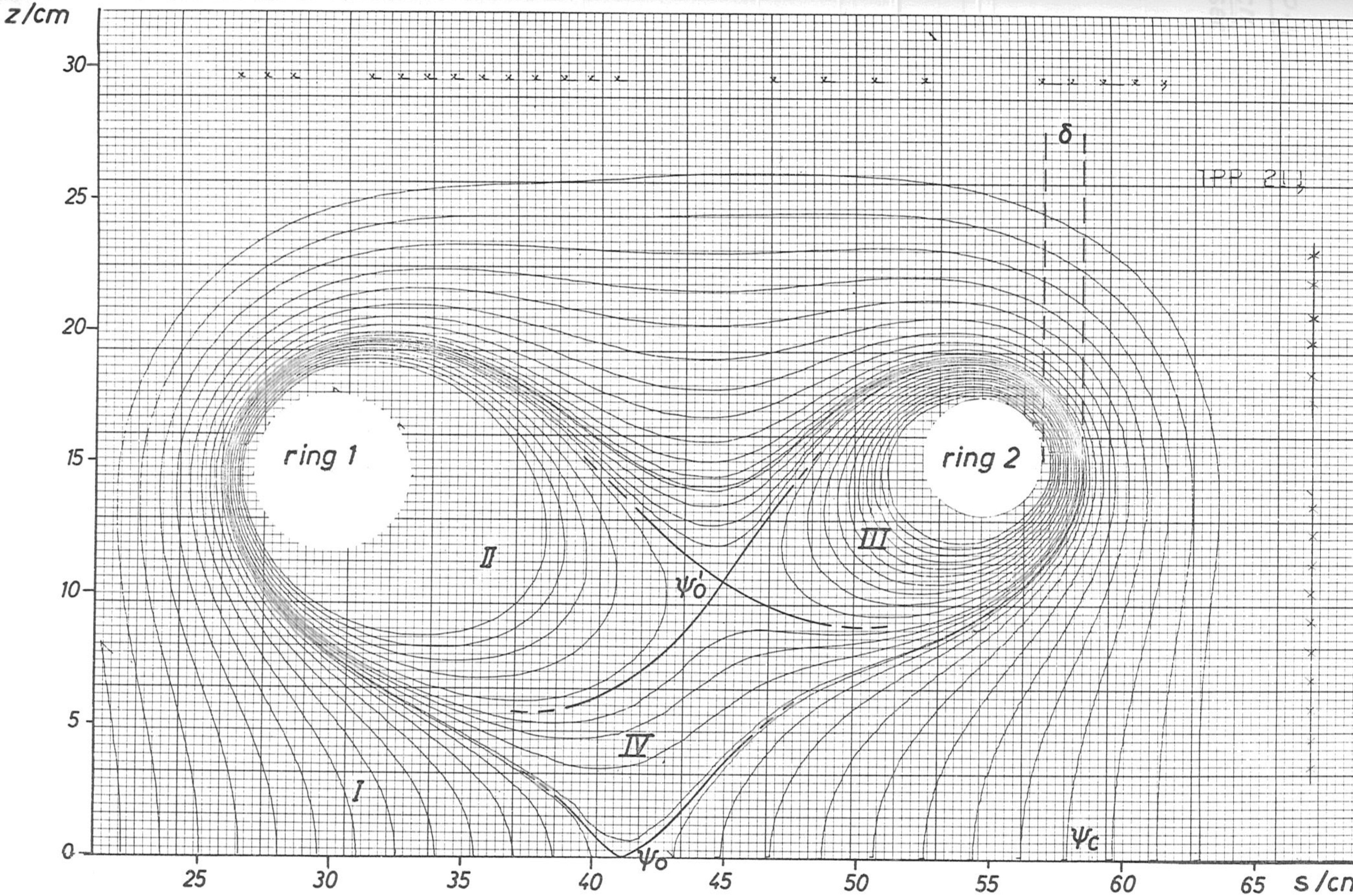
z/cm
30
25
20
15
10
5
0
25
30
35
40
45
50
55
60
65
s/cm
ring 1
ring 2
I
II
III
IV
δ
ψ_0'
ψ_0
ψ_c
IPP 2/1

Fig. 1

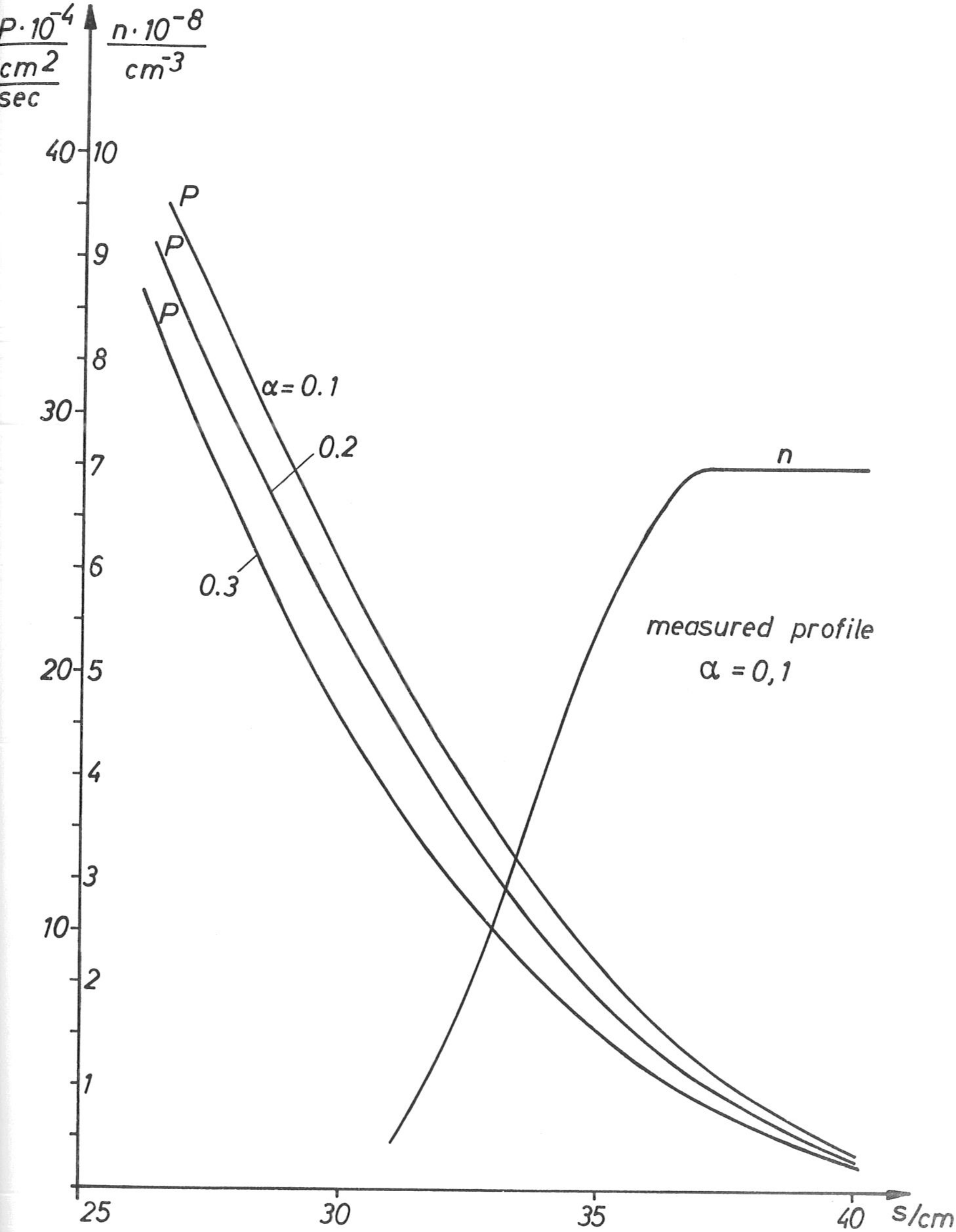

P·10⁻⁴ / cm2/sec
n·10⁻⁸ / cm⁻³
40
30
20
10
10
9
8
7
6
5
4
3
2
1
P
P
P
α= 0.1
0.2
0.3
n
measured profile
α =0,1
25
30
35
40
s/cm

Fig. 2

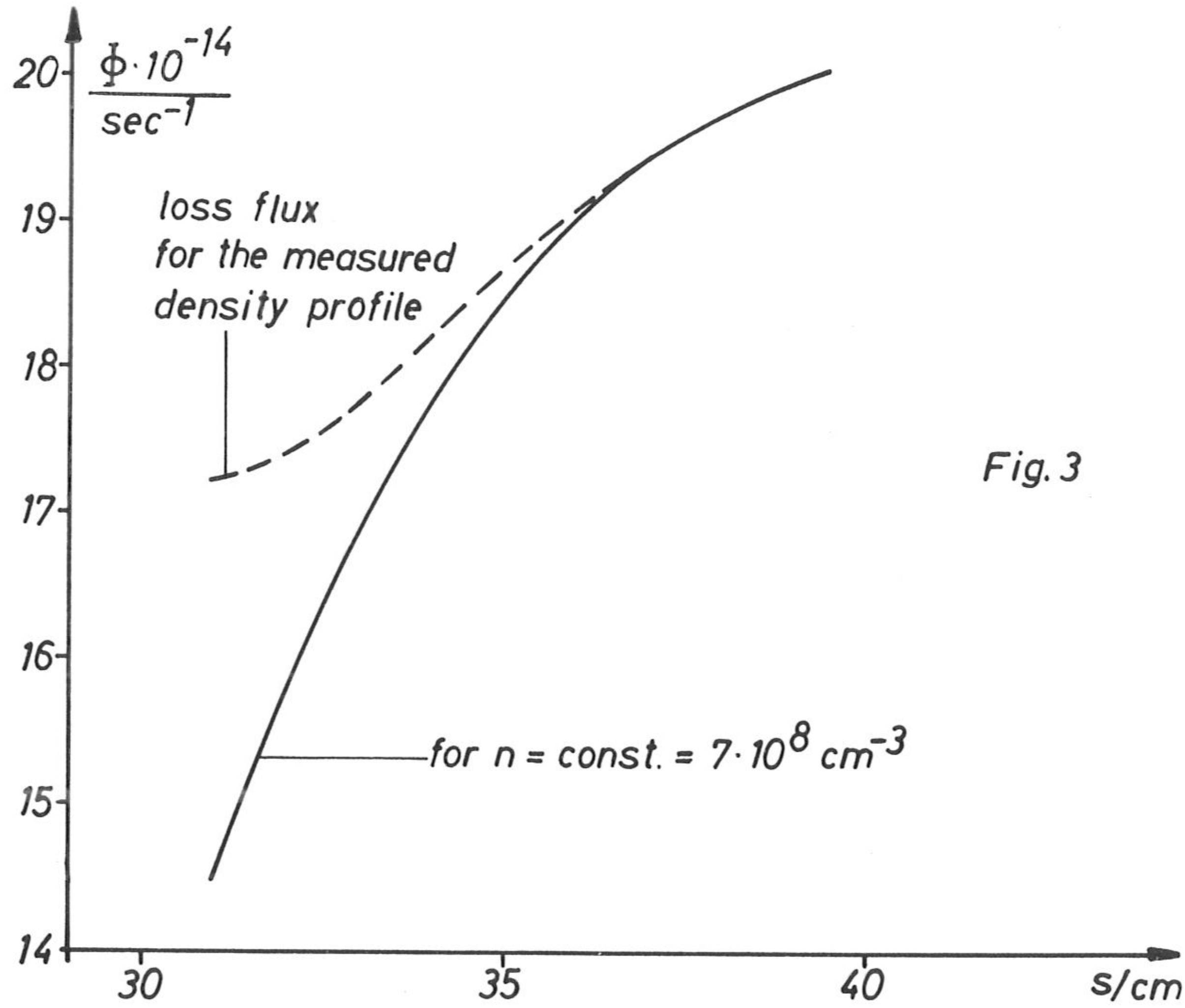

$\frac{\Phi \cdot 10^{-14}}{sec^{-1}}$
loss flux
for the measured
density profile
for n = const. = $7 \cdot 10^{8}$ cm^{-3}
20
19
18
17
16
15
14
30
35
40
s/cm

Fig. 3

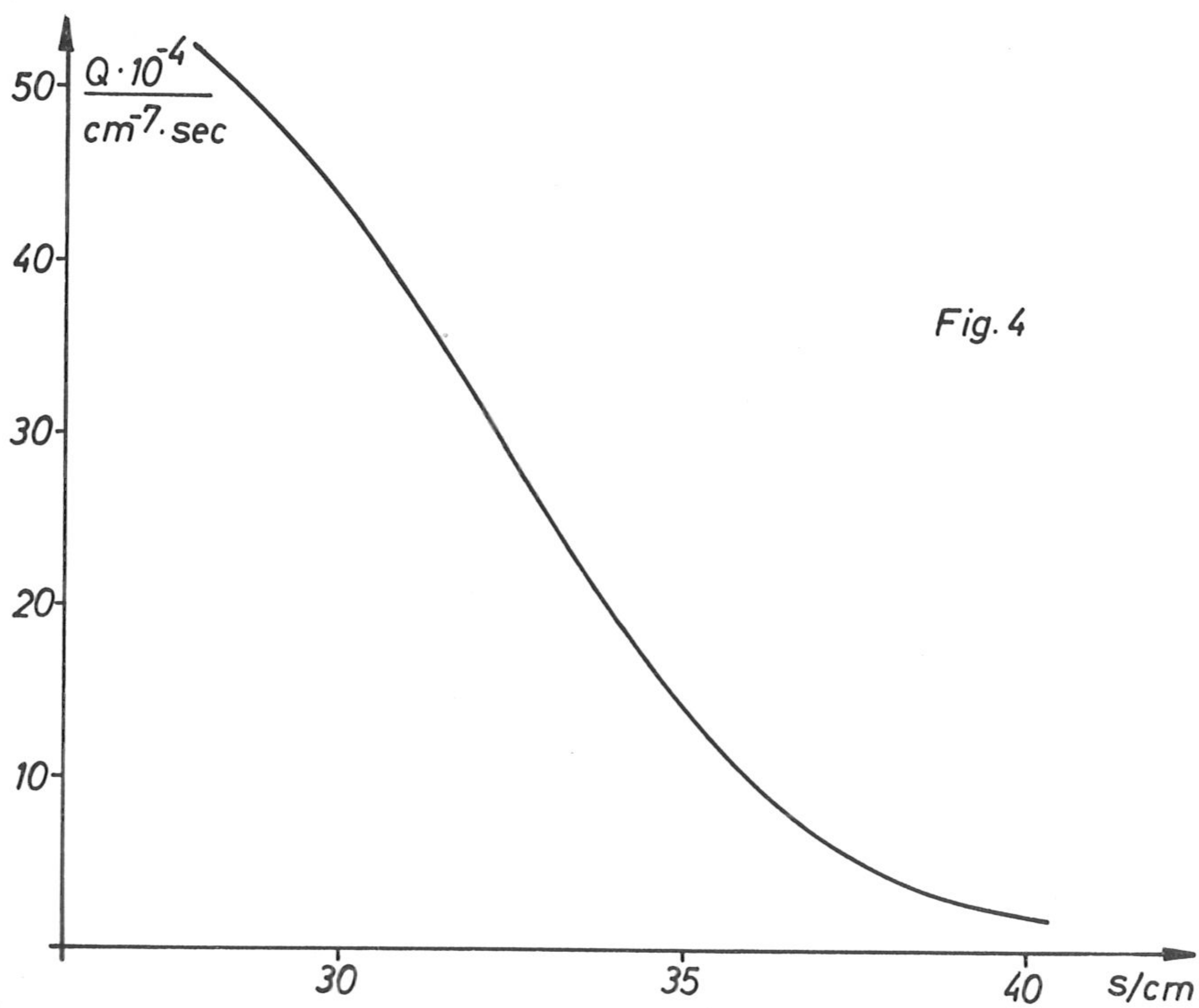

$\frac{Q \cdot 10^{-4}}{cm^{-7} \cdot sec}$
50
40
30
20
10
30
35
40
s/cm

Fig. 4

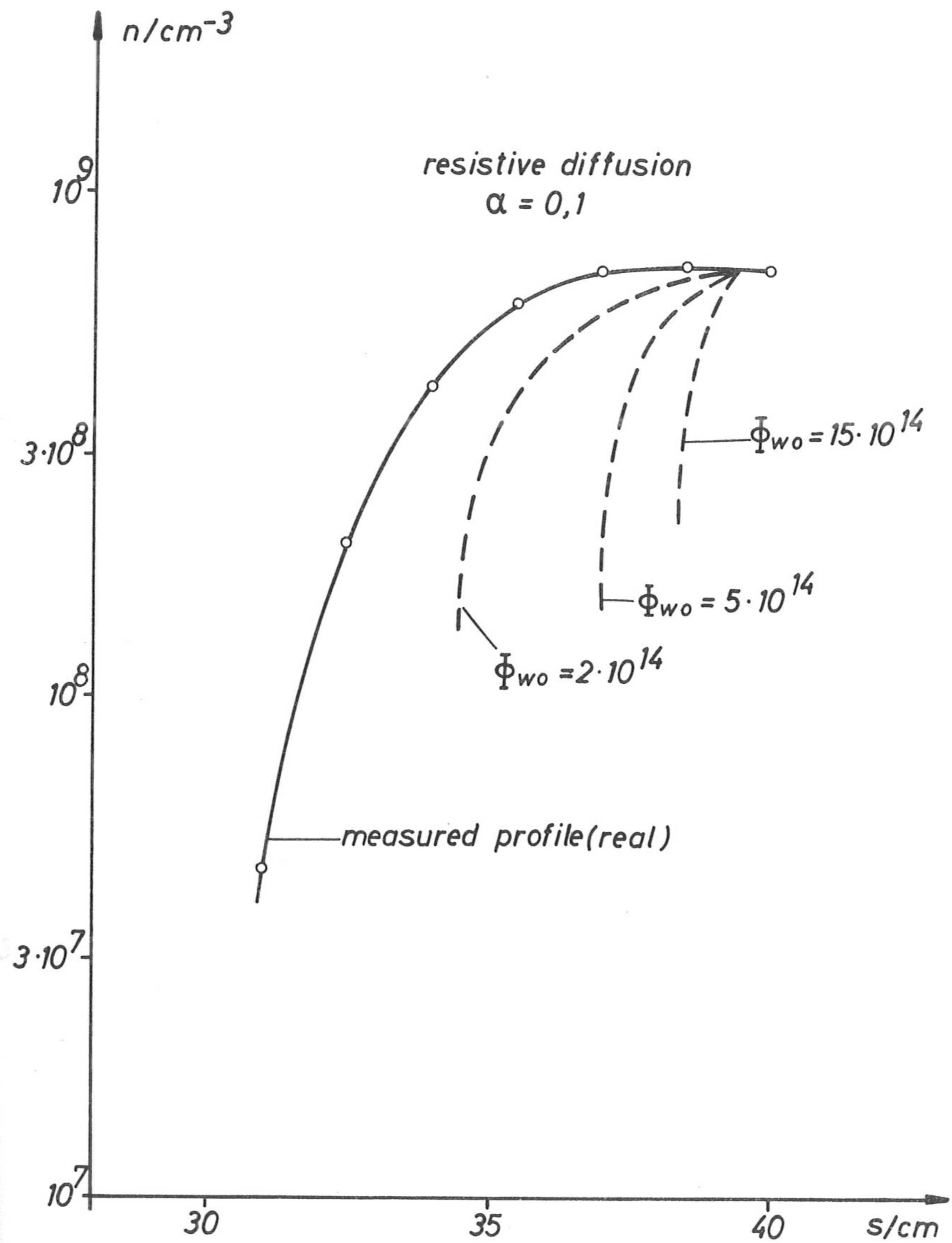

n/cm⁻³
resistive diffusion
α = 0,1
10⁹
3·10⁸
10⁸
3·10⁷
10⁷
Φwo = 15·10¹⁴
Φwo = 5·10¹⁴
Φwo = 2·10¹⁴
measured profile(real)
30
35
40
s/cm

Fig. 5

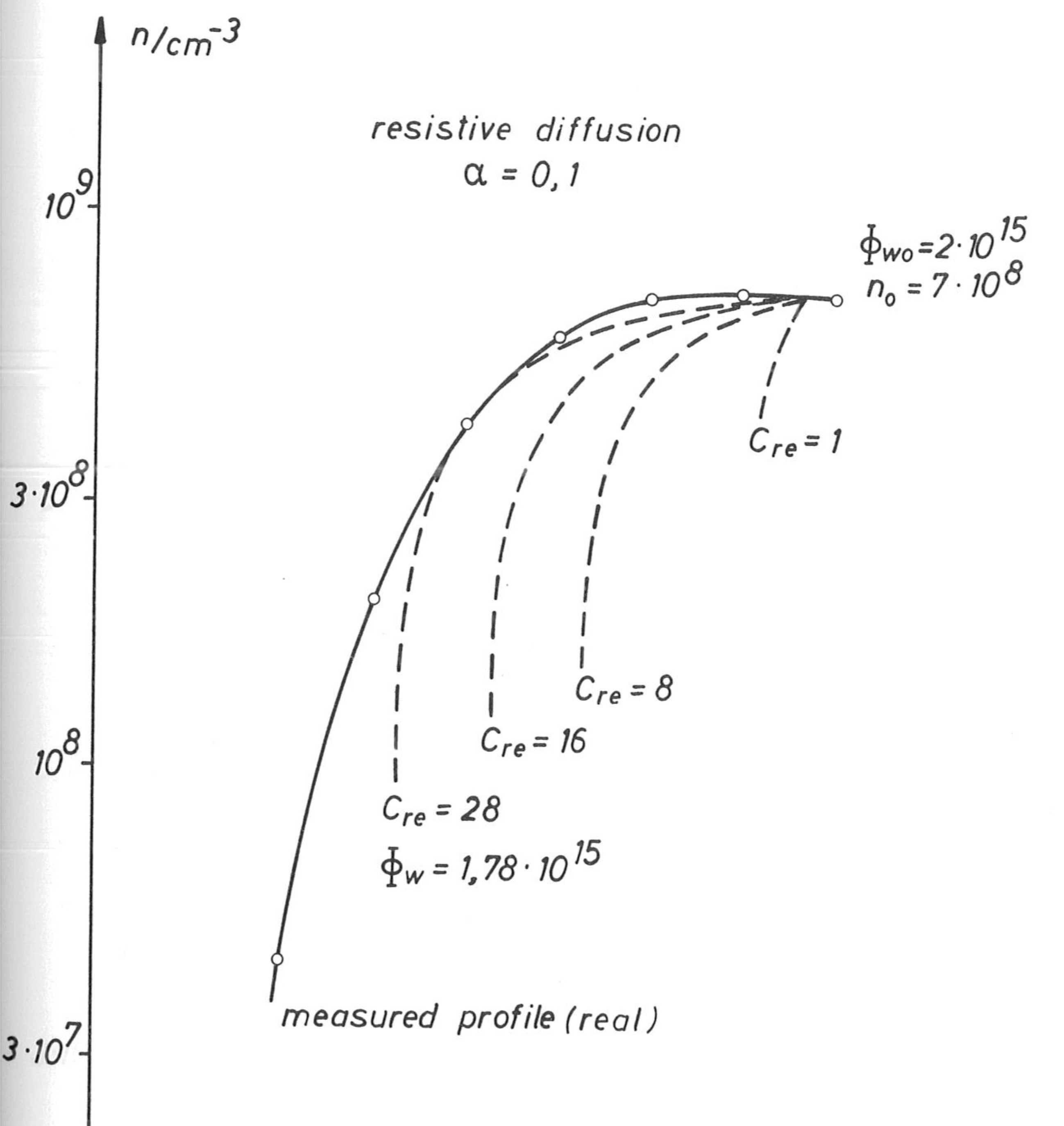

n/cm⁻³
resistive diffusion
α = 0,1
10⁹
3·10⁸
10⁸
3·10⁷
10⁷
Φwo = 2·10¹⁵
n₀ = 7·10⁸
Cre = 1
Cre = 8
Cre = 16
Cre = 28
Φw = 1,78·10¹⁵
measured profile (real)
30
35
40
s/cm

Fig. 6a

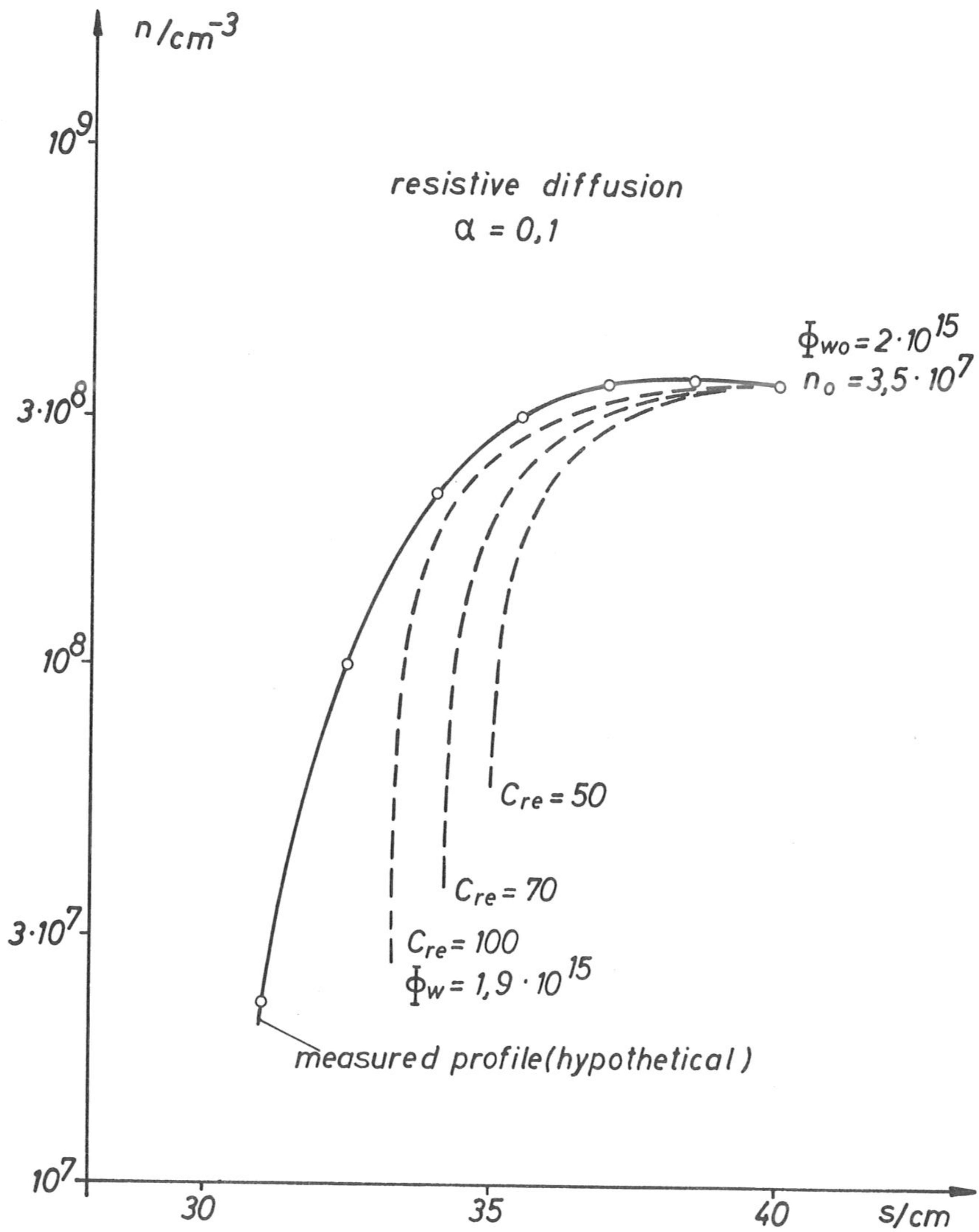
n/cm⁻³
10⁹
3·10⁸
10⁸
3·10⁷
10⁷
resistive diffusion
α = 0,1
Φwo = 2·10¹⁵
nₒ = 3,5·10⁷
Cre = 50
Cre = 70
Cre = 100
Φw = 1,9·10¹⁵
measured profile (hypothetical)
30
35
40
s/cm

Fig. 6b

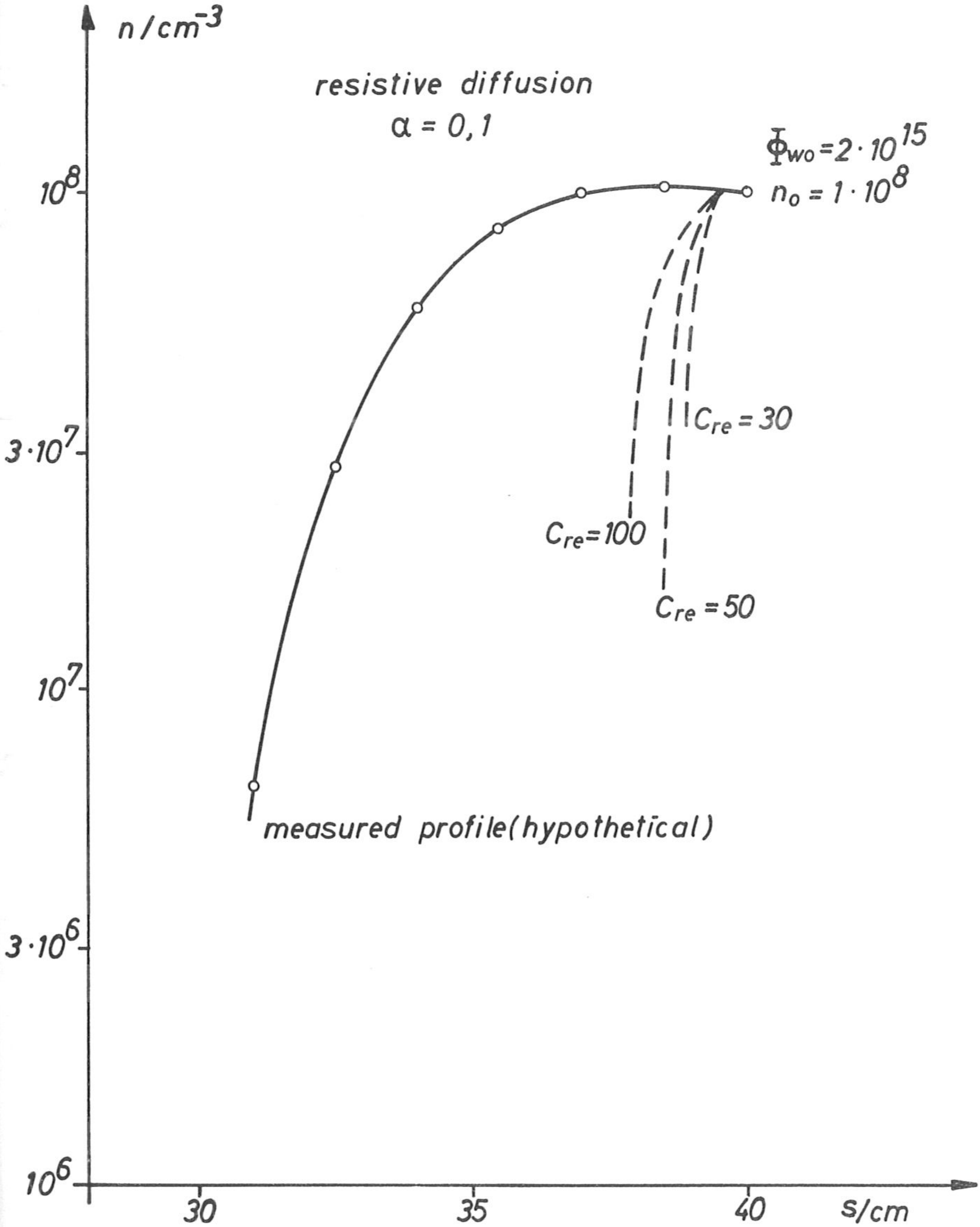
n/cm⁻³
resistive diffusion
α = 0,1
Φwo = 2 · 10^15
n₀ = 1 · 10^8
10^8
3 · 10^7
10^7
3 · 10^6
10^6
Cre = 30
Cre = 100
Cre = 50
measured profile (hypothetical)
30
35
40
s/cm

Fig. 6c

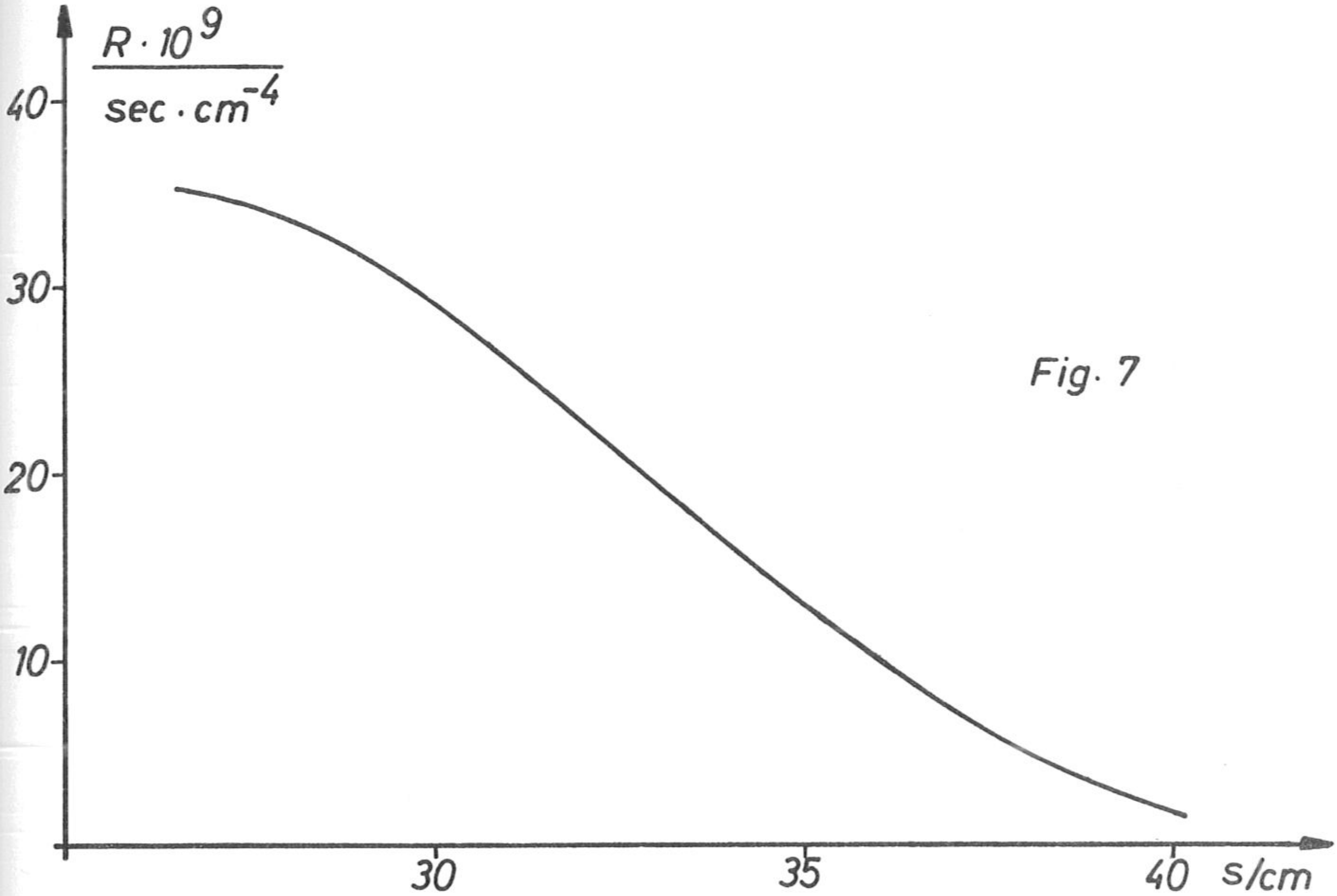

Fig. 7

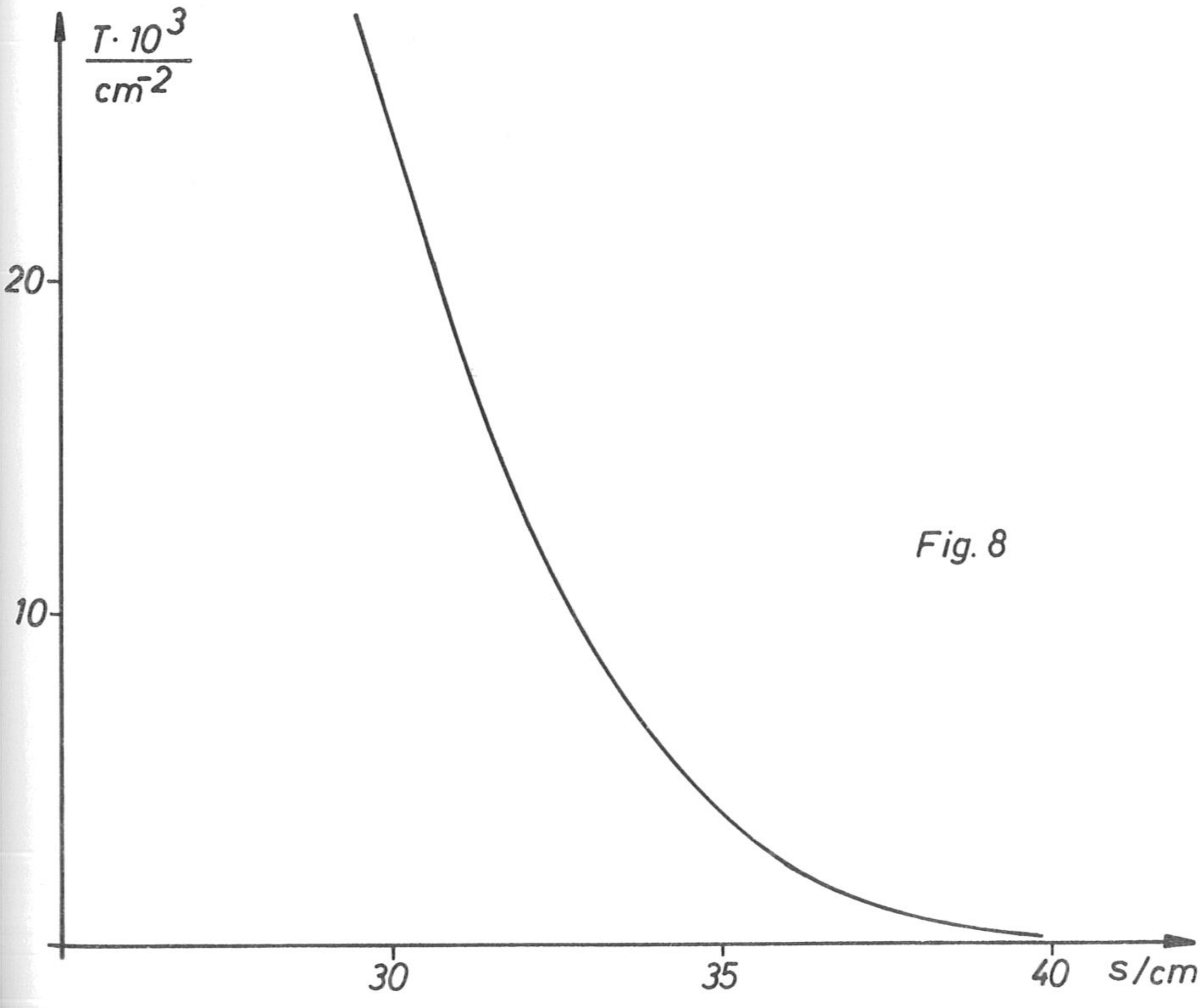

Fig. 8

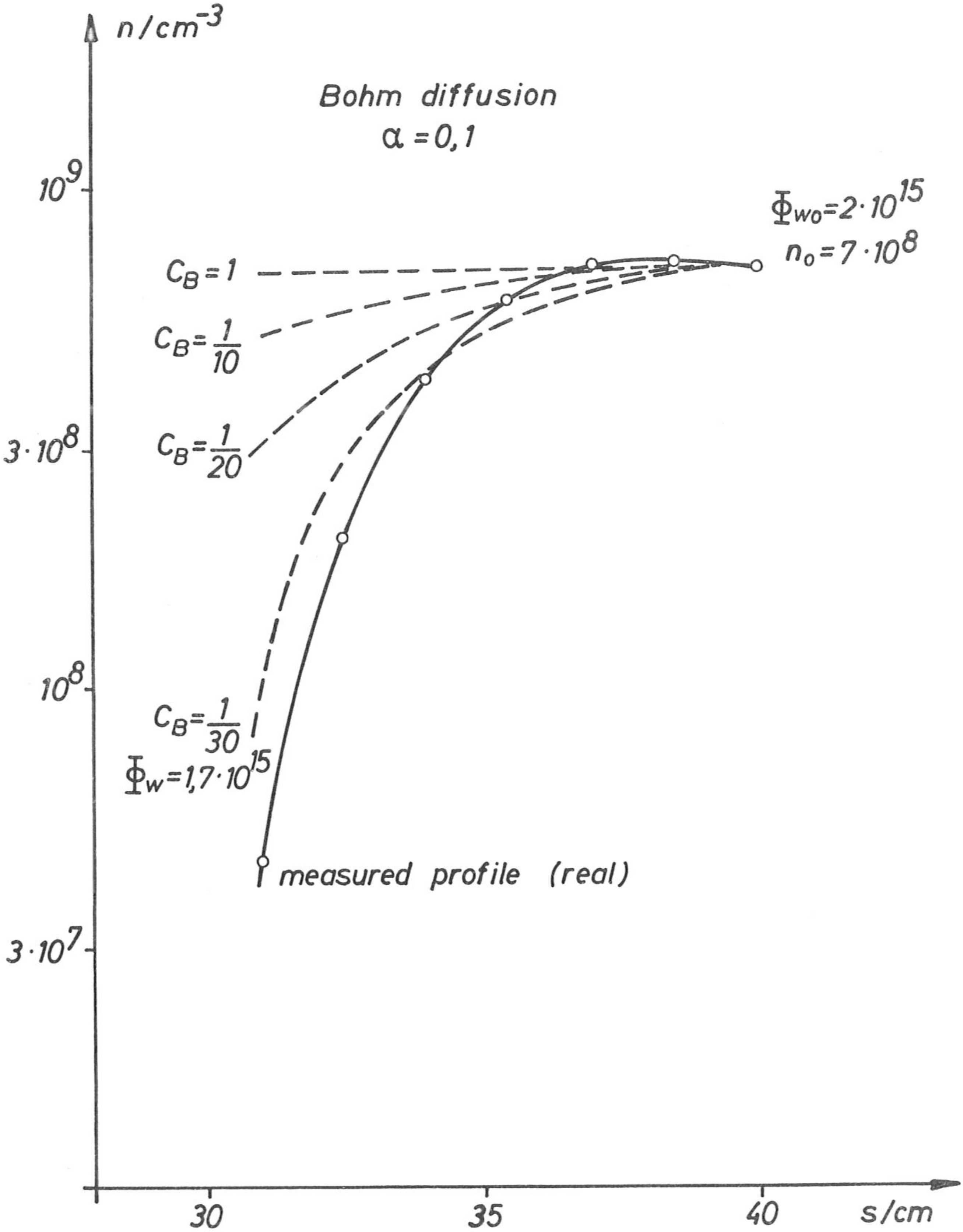
n/cm-3
Bohm diffusion
α = 0,1
10^9
3·10^8
10^8
3·10^7
Φwo=2·10^15
no=7·10^8
CB=1
CB=1/10
CB=1/20
CB=1/30
Φw=1,7·10^15
measured profile (real)
30
35
40
s/cm

Fig. 9a

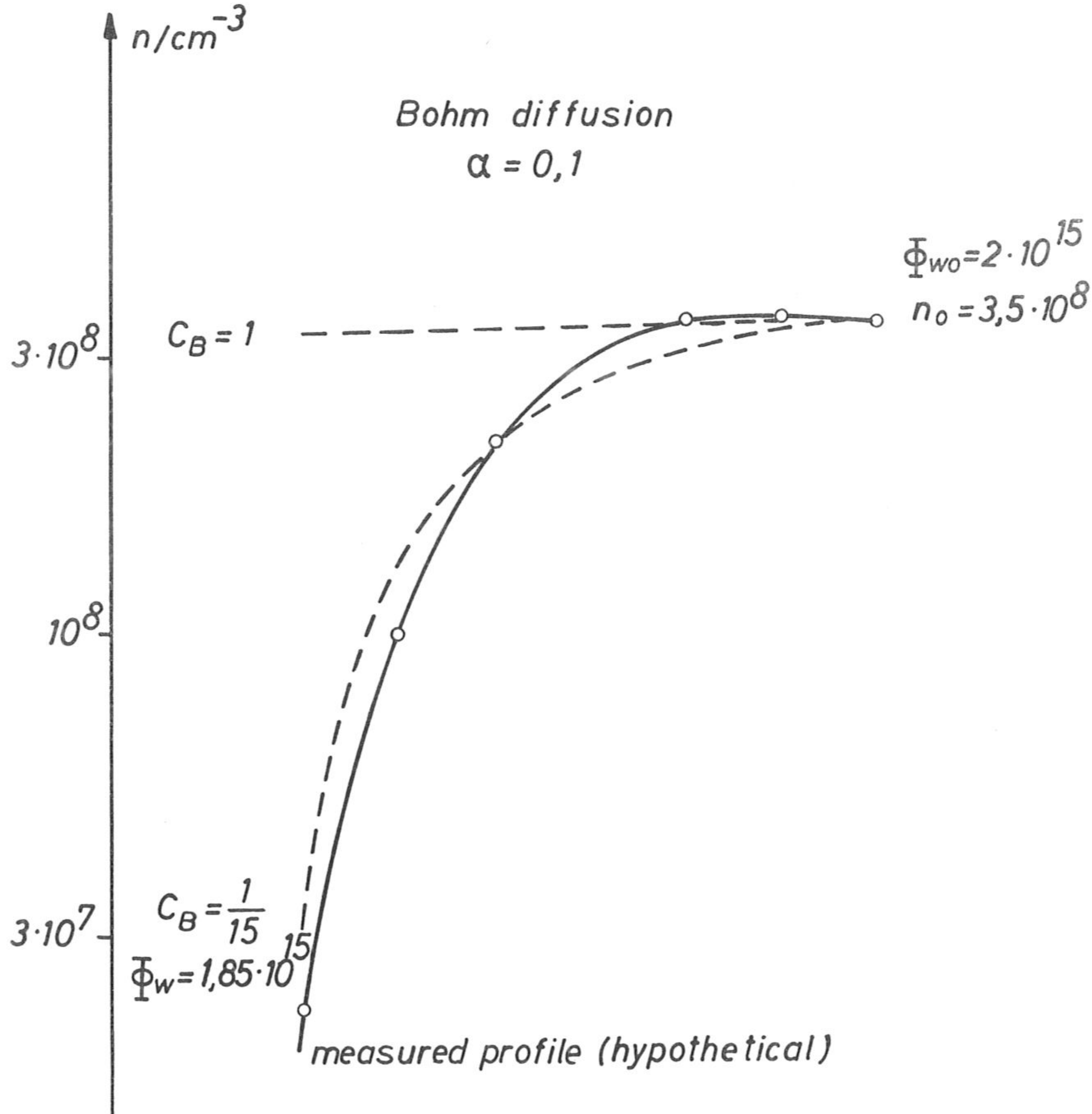

n/cm^-3
Bohm diffusion
α = 0,1
Φwo=2·10^15
n₀=3,5·10^8
C_B = 1
3·10^8
10^8
3·10^7
C_B = 1/15
Φw=1,85·10^15
measured profile (hypothetical)
30
35
40
s/cm

Fig. 9b

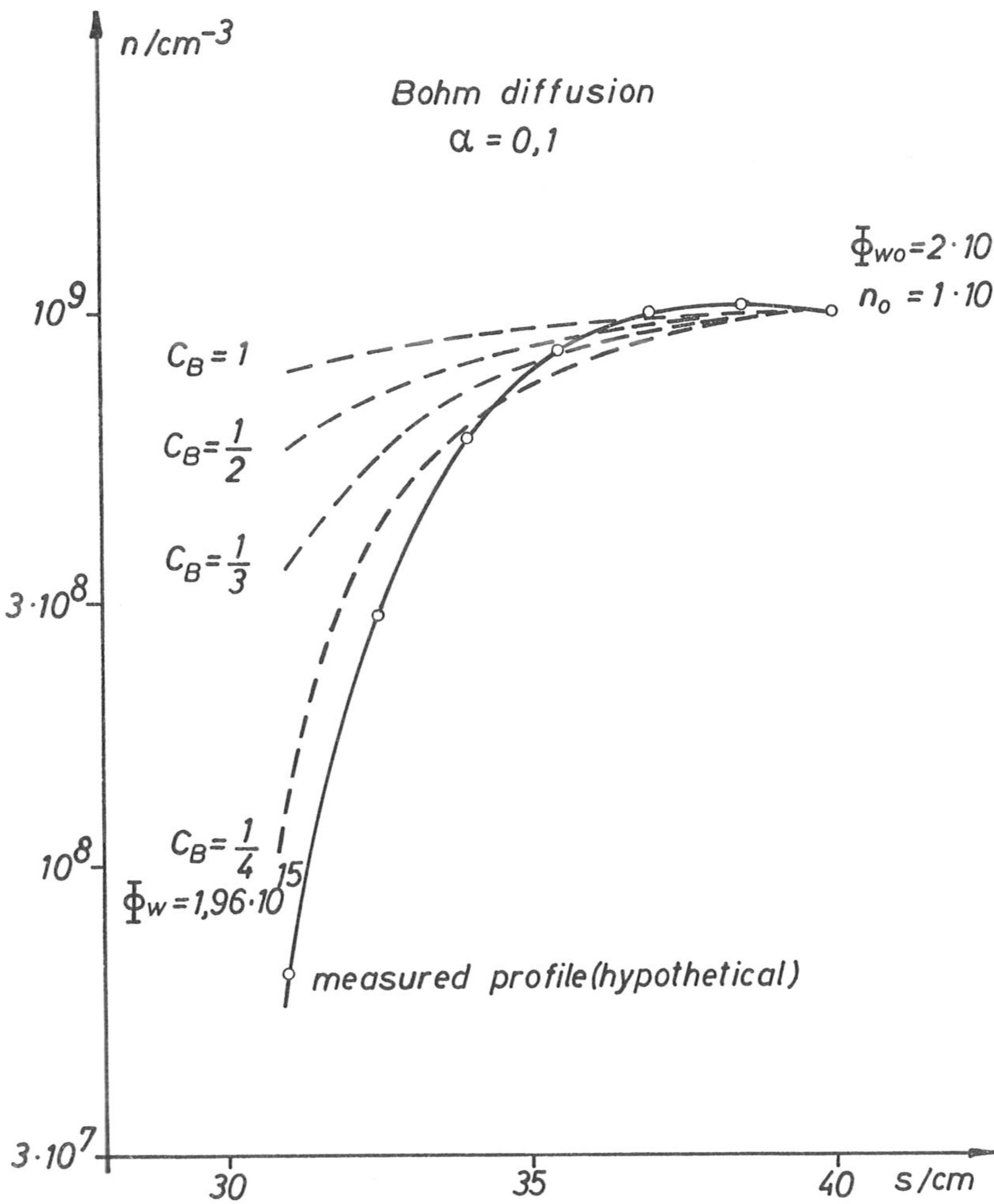
n /cm^-3
Bohm diffusion
α = 0,1
Φwo=2·10^15
no = 1·10^8
10^9
CB = 1
CB = 1/2
CB = 1/3
3·10^8
CB = 1/4
10^8
Φw = 1,96·10^15
measured profile (hypothetical)
3·10^7
30
35
40
s/cm

Fig. 9c

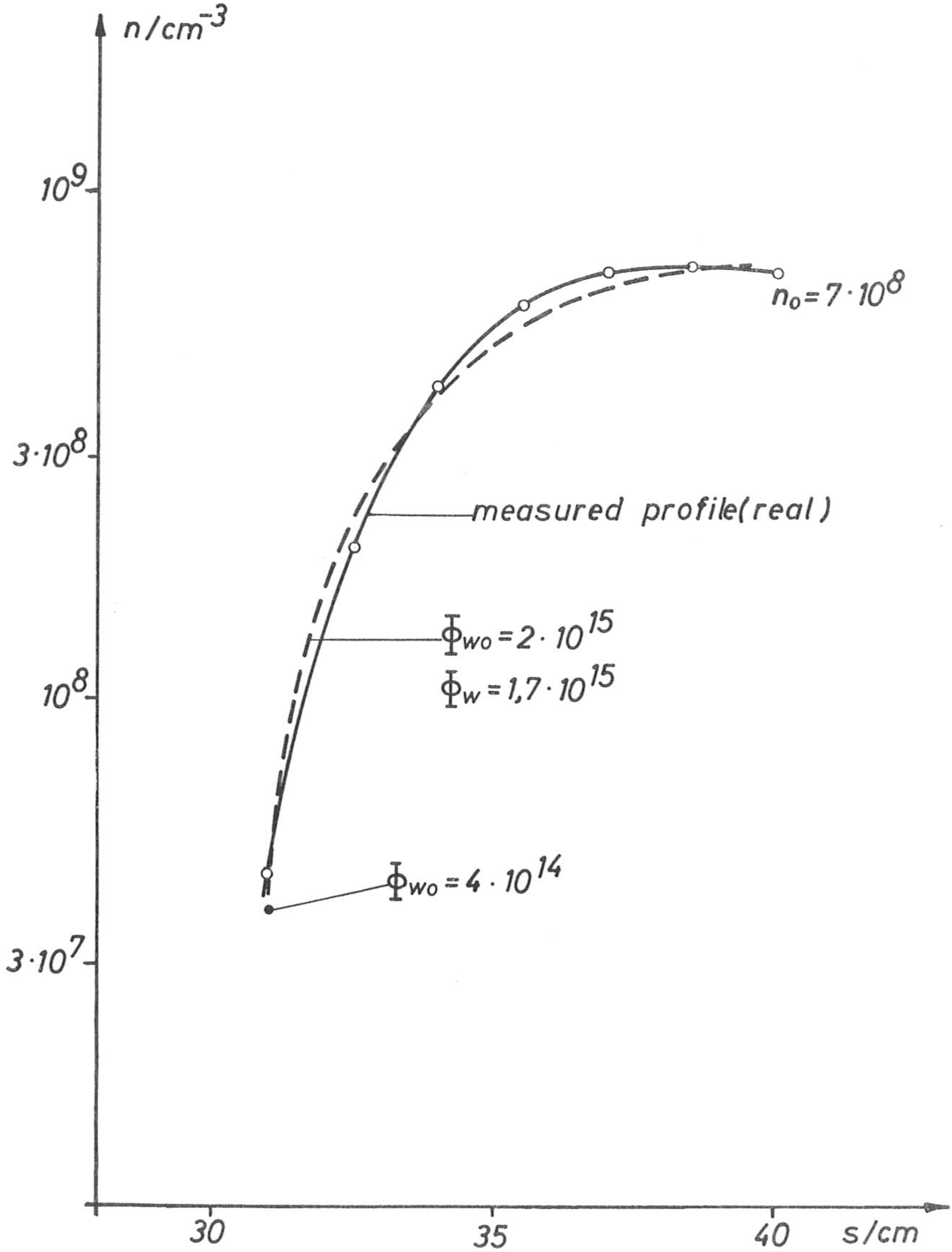
n/cm-3
10^9
3·10^8
10^8
3·10^7
n0=7·10^8
measured profile(real)
Φwo=2·10^15
Φw=1,7·10^15
Φwo=4·10^14
30
35
40
s/cm

Fig. 10